Supplementary Materials

Efficient Deep-Blue Electroluminescence Employing Heptazine-Based Thermally Activated Delayed Fluorescence

Jie Li [1], Jincheng Zhang [1], Heqi Gong [1], Li Tao [1], Yanqing Wang [2] and Qiang Guo [1,*]

[1]*College of Optoelectronic Engineering, Chengdu University of Information Technology, Chengdu 610225, China*

[2]*College of Polymer Science and Engineering, Sichuan University, Chengdu 610065, China*

**Correspondence: qiangguo@cuit.edu.cn*

Table of Contents

1. Instrumentation

NMR spectra were obtained on a Varian Inova 400 spectrometer. The ^{1}H NMR (400 MHz) and ^{13}C NMR (100 MHz) chemical shifts were measured relative to DMSO-d_6 as the internal reference (DMSO-d_6: δ = 2.50 ppm for ^{1}H and δ = 39.52 ppm for ^{13}C respectively). High-resolution mass spectra (HRMS) were obtained with Waters-Q-TOF-Premier (ESI^{+}). Elemental analysis was performed with a Yanaco MT-5 elemental analyzer. The UV and PL spectra were recorded with a Shimadzu UV-2550 spectrophotometer and Shimadzu RF-5301PC fluorescence spectrometer, respectively. The PLQY and transient PL decay were recorded using a Hamamatsu C9920-02 and a Hamamatsu C11367-03 measurement system, respectively. Transient PL decay characteristics of film samples under vacuum conditions were measured on a streak camera (C4334, Hamamatsu Photonics) equipped with cryostat using a YAG laser with an excitation wavelength of 355 nm. The highest occupied molecular orbital (HOMO) energy level of HAP-3DPA was determined by atmospheric ultraviolet photoelectron spectroscopy (AC-3E, Riken Keiki). The lowest unoccupied molecular orbital (LUMO) level was calculated by subtracting the energy gap from the HOMO level. Oxygen-free sample solutions (1×10^{-4} mol L^{-1}) were degassed with N_2 for 15 min prior to use unless otherwise indicated. Pure and doped films (100 nm) were deposited on quartz and silicon substrates by vacuum thermal evaporation at a pressure lower than 5×10^{-4} Pa.

2. Copies of ^{1}H and ^{13}C NMR spectra of HAP-3DPA

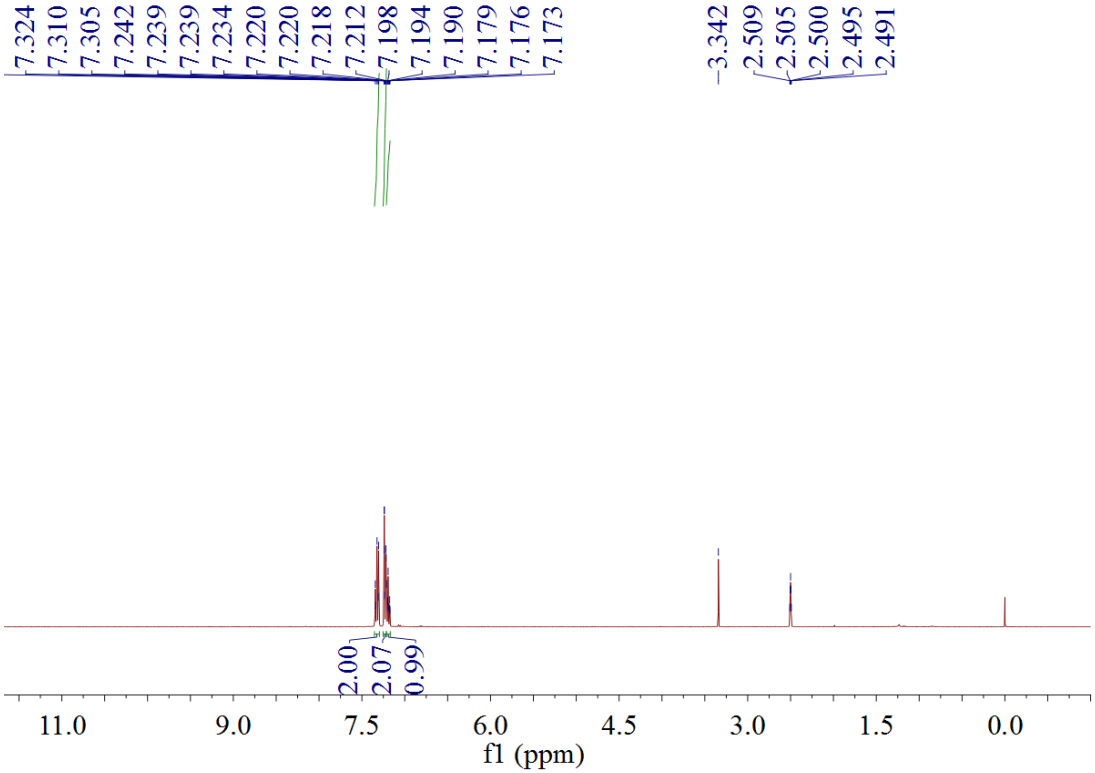

Figure S1. ^{1}H NMR spectrum of **HAP-3DPA** in DMSO-d_6.

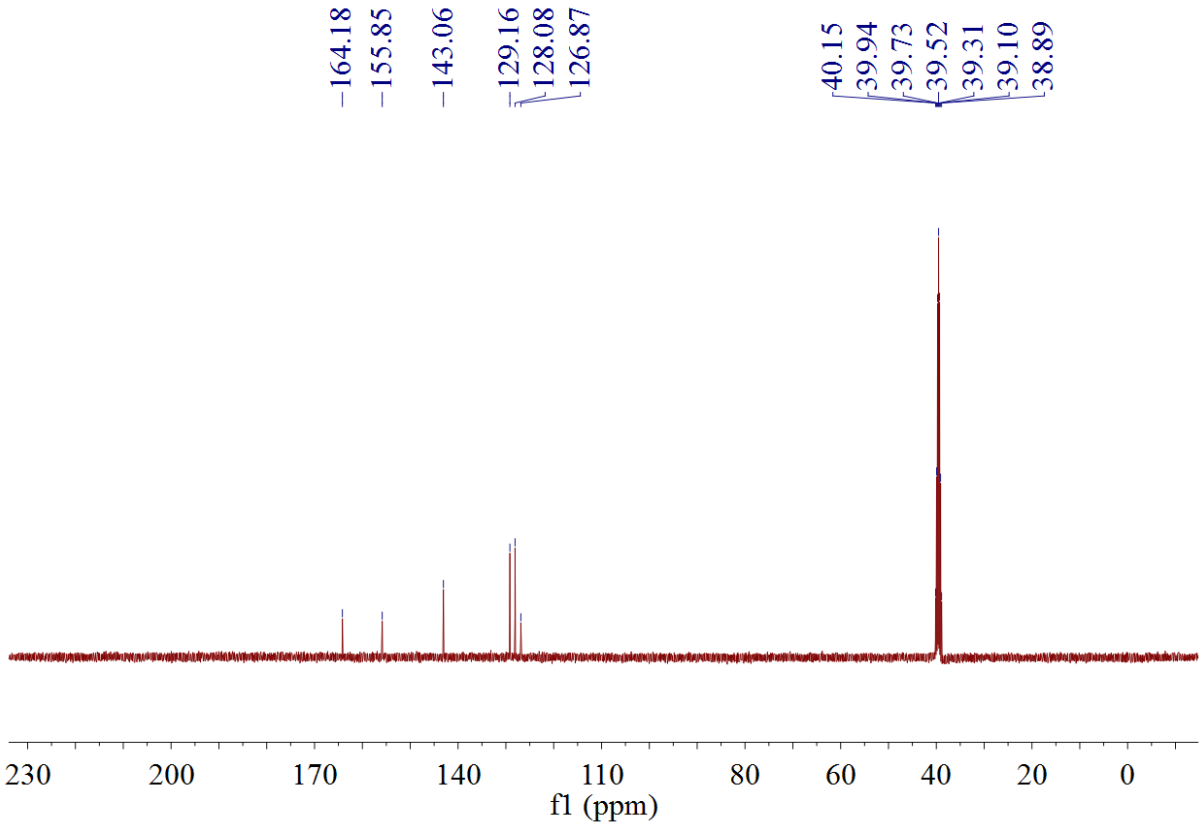

Figure S2. ^{13}C NMR spectrum of **HAP-3DPA** in DMSO-d_6.

3. Quantum Chemical Calculations

All calculations were performed using the Gaussian 09 program package. The HOMO and LUMO of HAP-3DPA and 4,4,4″-(1,3,3a[1],4,6,7,9-heptaazaphenalene-2,5,8-triyl)tris(*N*, *N*-bis(4-(*tert*-butyl)phenyl)aniline) (HAP-3TPA) were calculated using the nonlocal density functional of Becke's 3-parameters employing Lee-Yang-Parr functional (B3LYP) with the 6-31G(d) basis set. Their S_1 and T_1 were calculated by the time-dependent density functional theory (TD-DFT) method at the optimized ground-state geometries using the B3LYP mode with a 6-31G(d) basis set [S1].

3.1 The Optimized Geometry Data for HAP-3DPA (unit: Å)

C	7.09961	1.47268	0.09892
C	6.97458	0.58702	-0.97246
C	5.88263	-0.27728	-1.04483
C	4.91002	-0.26081	-0.04034
C	5.0367	0.62	1.03838
C	6.12691	1.48609	1.10084
N	3.82158	-1.20168	-0.10998
C	2.51016	-0.7897	-0.07372

N	2.29899	0.53927	-0.08337
C	1.03757	0.95134	-0.04376
N	0.00053	-0.00126	-0.00503
C	0.30736	-1.37553	-0.00278
N	1.57809	-1.75888	-0.0299
N	0.73369	2.24367	-0.04691
C	-0.57179	2.56641	-0.00451
N	-1.61694	1.71953	0.03483
C	-1.34292	0.42066	0.03045
N	-2.30961	-0.48861	0.06941
C	-1.93563	-1.781	0.06401
N	-0.67973	-2.26265	0.02702
N	-0.87098	3.90832	-0.00022
N	-2.94821	-2.7108	0.10097
C	-2.67981	-4.11993	0.22479
C	-4.33167	-2.31889	0.02082
C	0.1578	4.91235	0.08172
C	-2.23031	4.37855	-0.07392
C	-2.69701	5.25353	0.91191
C	-3.99272	5.76331	0.83563
C	-4.82876	5.40103	-0.22152
C	-4.35941	4.52795	-1.20511
C	-3.06301	4.02054	-1.13897
C	-5.20922	-2.72609	1.03012
C	-6.56316	-2.40229	0.94961
C	-7.04681	-1.66937	-0.13511
C	-6.16804	-1.26546	-1.1426
C	-4.81503	-1.59233	-1.07201
C	-3.24782	-4.99957	-0.70246
C	-3.04608	-6.37342	-0.57519
C	-2.27439	-6.87622	0.47334
C	-1.70904	-5.99548	1.39794
C	-1.91337	-4.62177	1.28181
C	0.19748	5.9191	-0.88795

C	1.1509	6.93316	-0.80252
C	2.07091	6.94575	0.24675
C	2.02861	5.93914	1.21382
C	1.07317	4.92724	1.13917
C	4.17518	-2.59338	-0.21804
C	3.70094	-3.38198	-1.27126
C	4.09748	-4.71439	-1.37164
C	4.97436	-5.26501	-0.43467
C	5.45304	-4.47315	0.61008
C	5.05452	-3.14152	0.72132
H	7.9492	2.14773	0.15363
H	7.72486	0.56935	-1.75821
H	5.78054	-0.96971	-1.87472
H	4.27782	0.63255	1.81224
H	6.21706	2.17122	1.93936
H	-2.04187	5.53245	1.73127
H	-4.34851	6.44063	1.60714
H	-5.83909	5.79645	-0.27979
H	-5.00317	4.24192	-2.03239
H	-2.69843	3.33852	-1.89854
H	-4.82741	-3.29658	1.87117
H	-7.23797	-2.72022	1.73968
H	-8.10136	-1.4151	-0.19594
H	-6.5364	-0.69615	-1.99161
H	-4.12987	-1.27596	-1.85023
H	-3.84816	-4.60359	-1.51566
H	-3.49007	-7.04937	-1.30092
H	-2.11504	-7.94658	0.57062
H	-1.10788	-6.3776	2.21838
H	-1.47059	-3.93731	1.99604
H	-0.52124	5.90475	-1.70133
H	1.17581	7.71038	-1.56144
H	2.8157	7.73417	0.31138
H	2.7397	5.94233	2.03538

H 1.04128 4.14327 1.88712

H 3.01565 -2.9557 -1.99478

H 3.72044 -5.32259 -2.18921

H 5.28284 -6.30337 -0.51914

H 6.13531 -4.89106 1.34537

H 5.4255 -2.52065 1.53099

3.2 Excitation Energies and Oscillator Strengths for HAP-3DPA

Excited State 1: Triplet-A 3.3009 eV 375.61 nm f=0.0000 <S**2>=2.000

174 ->179 0.15161

175 ->177 0.12811

175 ->178 -0.13741

176 ->177 0.57976

176 ->179 0.10605

Excited State 2: Triplet-A 3.3036 eV 375.30 nm f=0.0000 <S**2>=2.000

174 ->178 0.14743

175 ->177 0.57820

175 ->179 -0.12001

176 ->177 -0.12890

176 ->178 -0.13352

Excited State 3: Triplet-A 3.3776 eV 367.08 nm f=0.0000 <S**2>=2.000

174 ->177 0.52934

175 ->178 0.21447

176 ->179 0.22879

Excited State 4: Triplet-A 3.5088 eV 353.35 nm f=0.0000 <S**2>=2.000

173 ->177 0.56817

174 ->180 0.15211

175 ->179 -0.12549

175 ->182 -0.14561

176 ->178 0.12332

176 ->181 0.14670

Excited State 5: Singlet-A 3.5385 eV 350.39 nm f=0.0000 <S**2>=0.000

173 ->177 0.69074

Excited State 6: Singlet-A 3.6255 eV 341.98 nm f=0.3979 <S**2>=0.000

176 ->177 0.68922

Excited State	7:	Singlet-A	3.7400 eV	331.50 nm	f=0.4328 <S**2>=0.000
175 ->177	0.69156				
Excited State	8:	Singlet-A	3.7513 eV	330.51 nm	f=0.0015 <S**2>=0.000
164 ->177	-0.13631				
170 ->177	-0.12743				
174 ->177	0.66681				

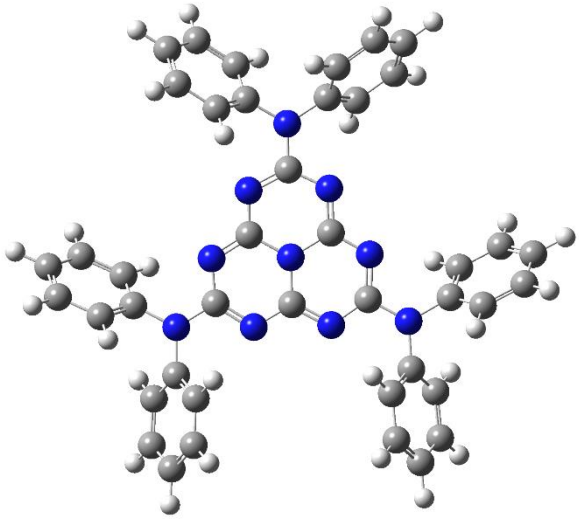

Figure S3. The optimized geometry of the ground state of HAP-3DPA by theoretical calculations.

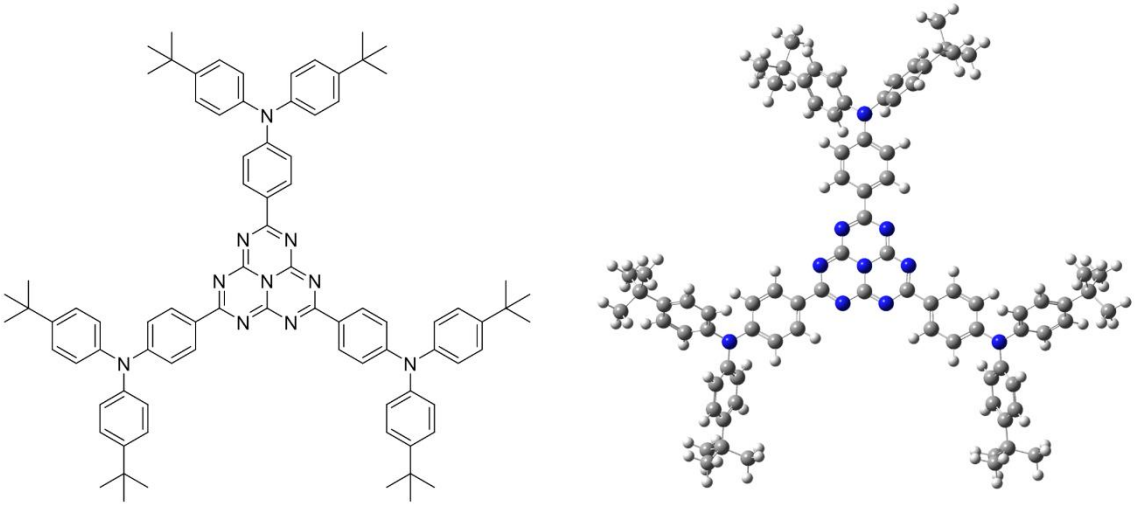

Figure S4. Molecular structure (left), and optimized geometry of the ground state (right) of HAP-3TPA by theoretical calculations.

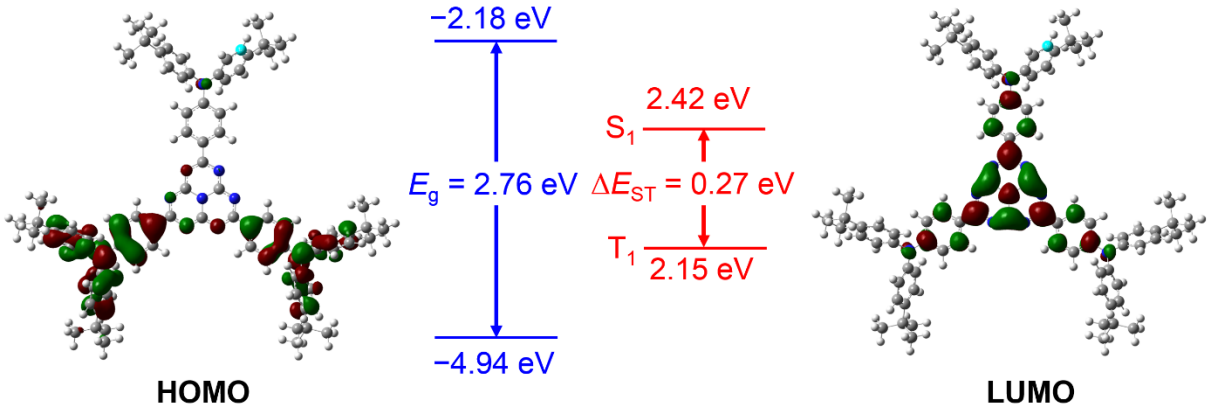

Figure S5. Frontier molecular orbital distributions and energy levels of the lowest excited singlet and triplet states of HAP-3TPA by theoretical calculations.

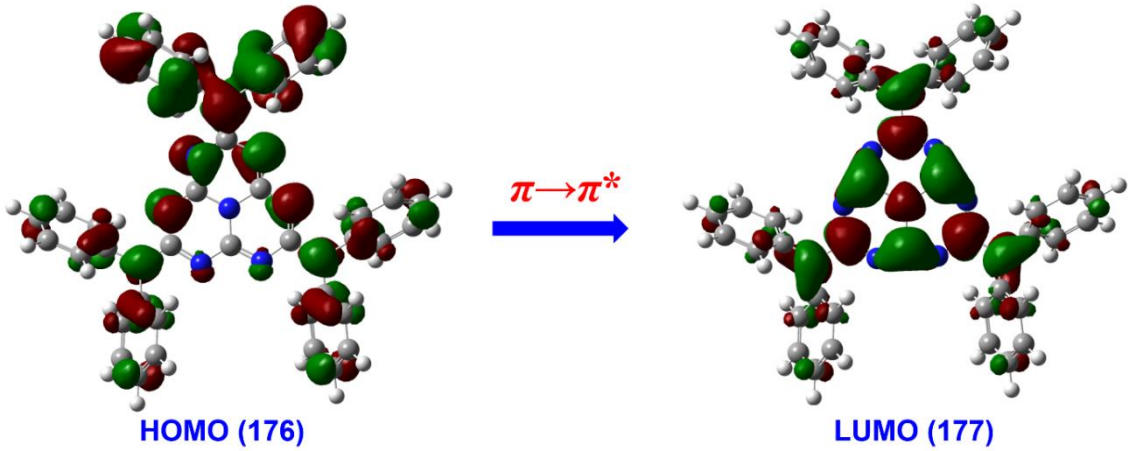

Figure S6. The natural transition orbitals (176 ->177) for the lowest excited triplet state (T_1) of HAP-3DPA by theoretical calculations.

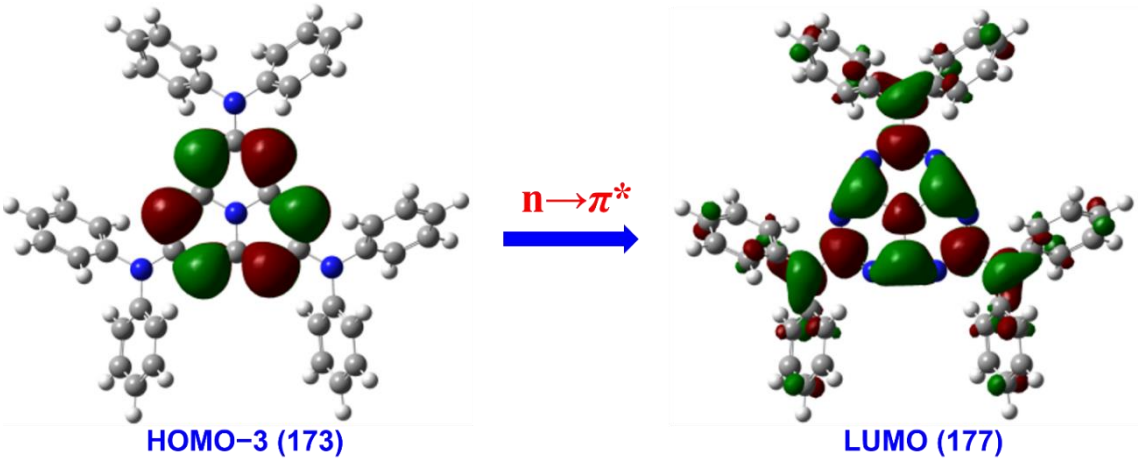

Figure S7. The natural transition orbitals (173 ->177) for the lowest excited singlet state (S_1) of HAP-3DPA by theoretical calculations.

4. Photophysical Properties

Table S1. The PLQYs of HAP-3DPA in DPEPO doped films at various concentrations.

Concentration	PLQY
2 wt% HAP-3DPA:DPEPO	64%
6 wt% HAP-3DPA:DPEPO	67%
10 wt% HAP-3DPA:DPEPO	60%

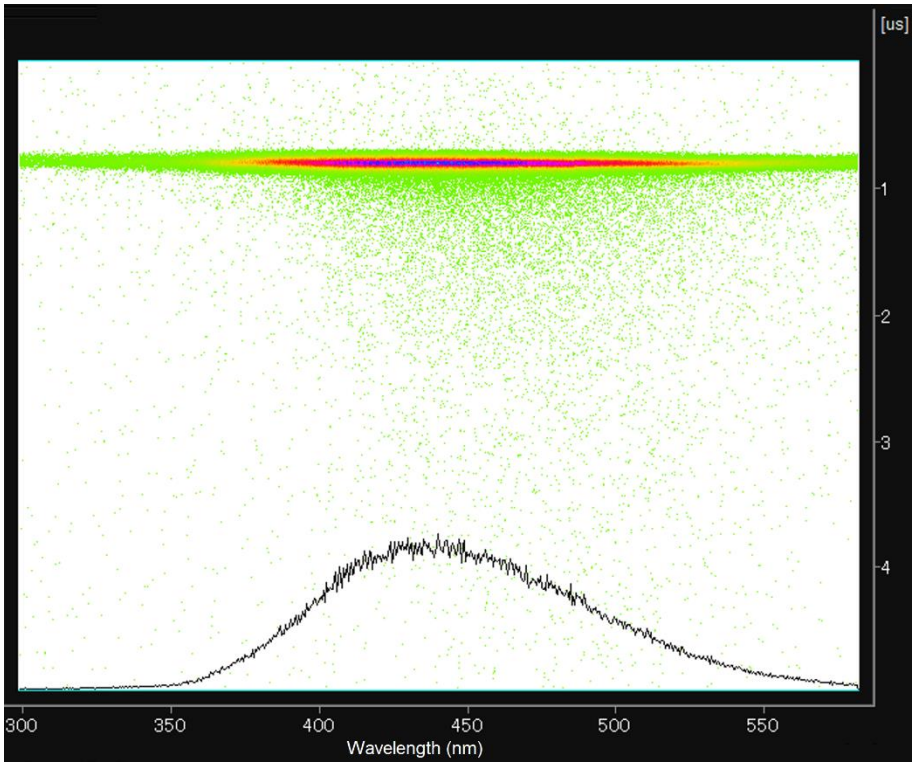

Figure S8. The transient PL decay image of 6 wt% HAP-3DPA:DPEPO doped film in the time range of 5 μs.

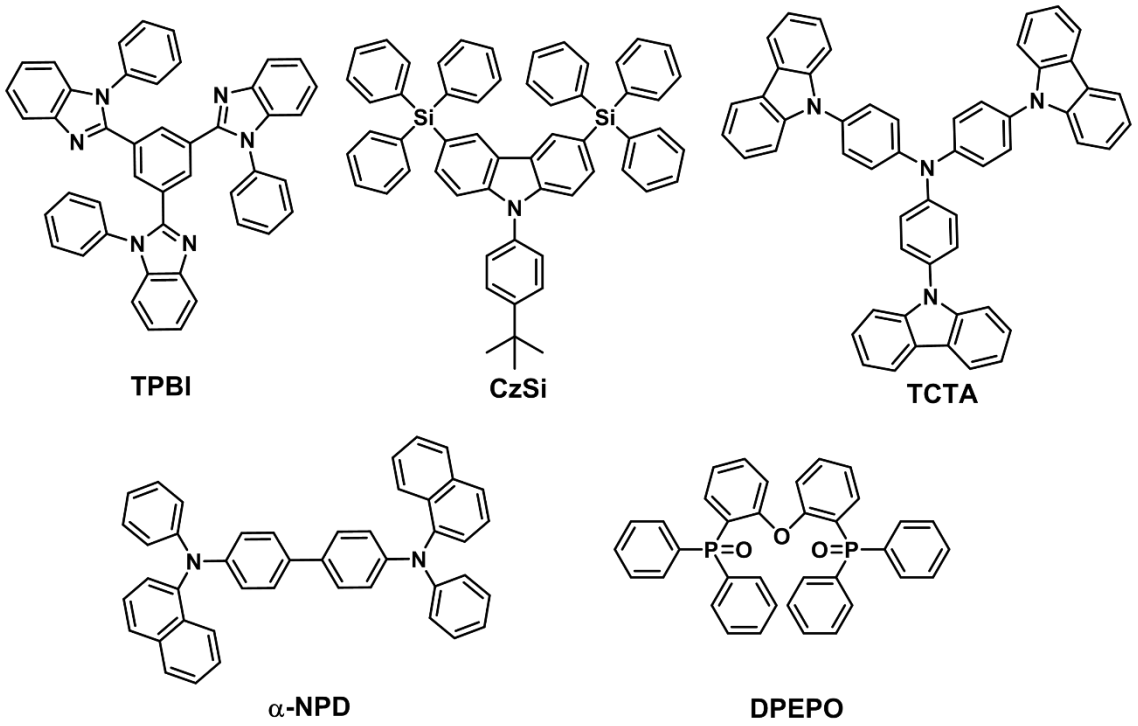

Figure S9. The molecular structures of organic compounds used in the OLED device.

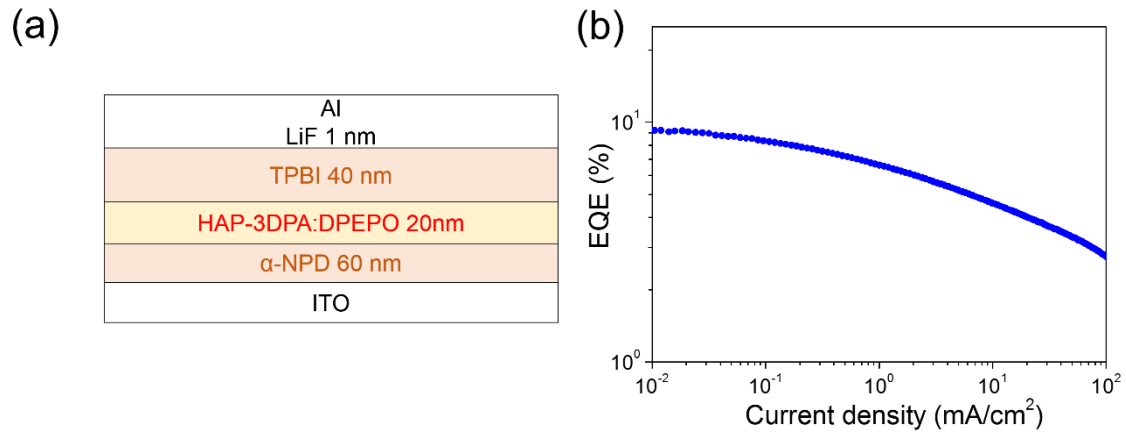

Figure S10. (**a**) The three-layered OLED structure. (**b**) EQE as a function of current density.

Table S2. The EL performance of three-layered OLED based on HAP-3DPA.

Emitter	V_{on} (V)[a]	λ_{EL} (nm)	L_{max} (cd m^{-2})	EQE (%)	CIE (x, y)
HAP-3DPA	4.0	441	8760	9.5	0.16, 0.13

[a] Turn-on voltage at 1 cd m^{-2}.

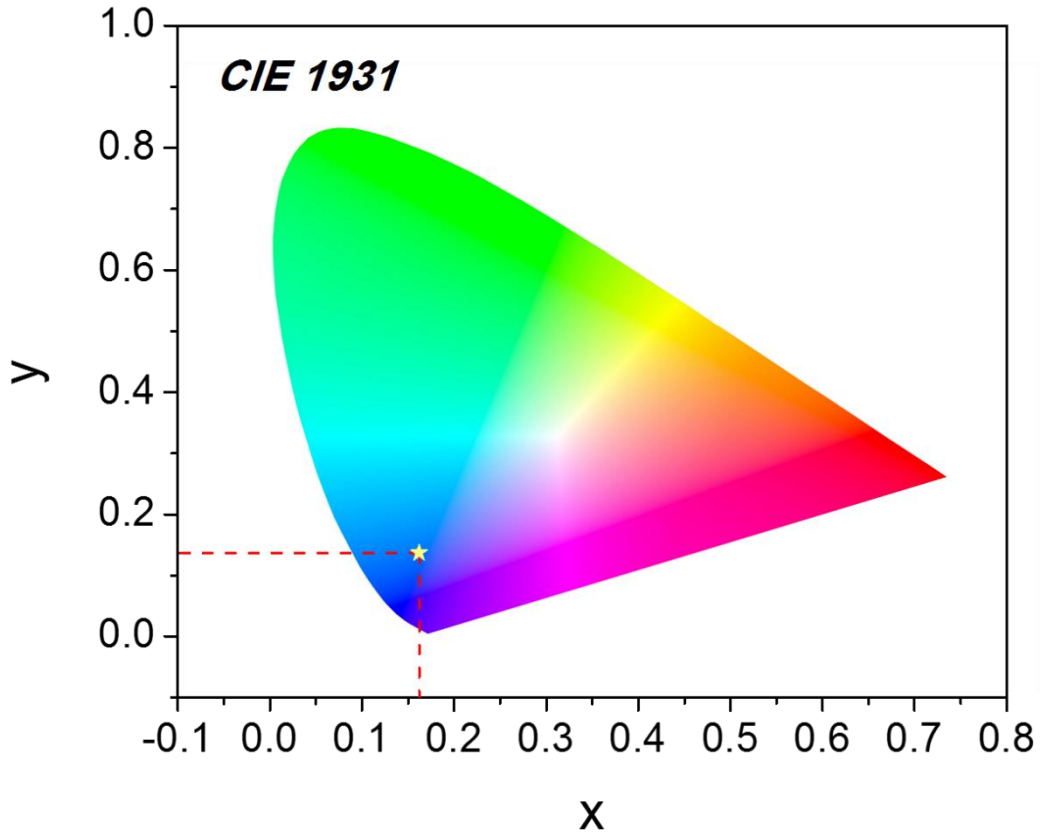

Figure S11. The Commission Internationale de l'Eclairage (CIE) coordinates of (0.16, 0.13) for HAP-3DPA.

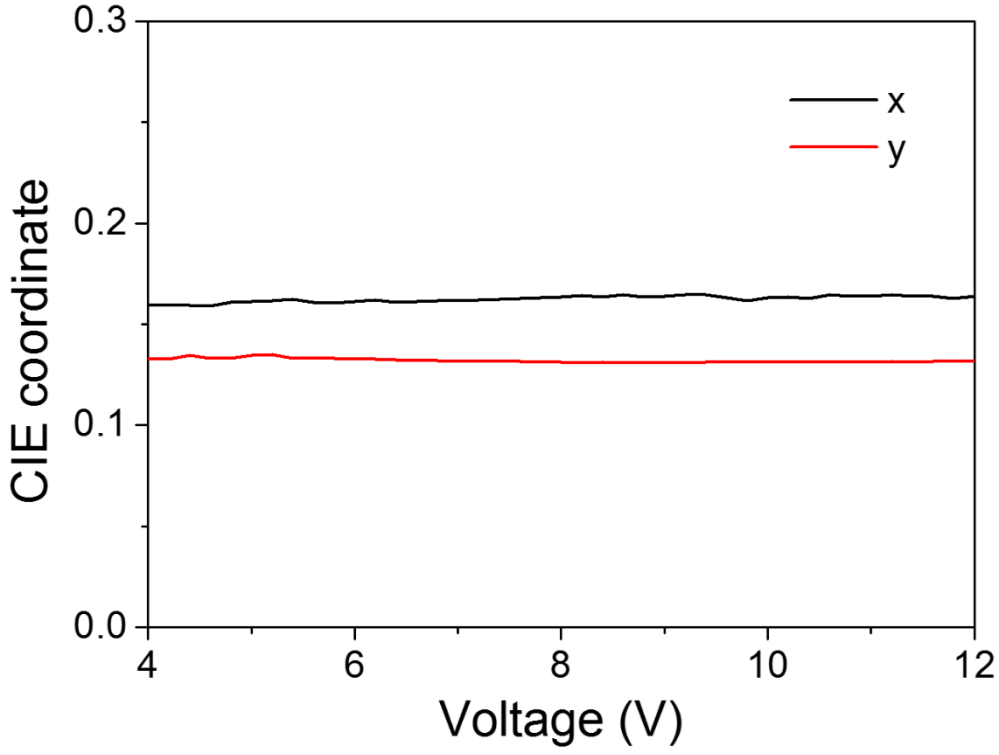

Figure S12. The CIE coordinates of HAP-3DPA based OLED with applied voltage increasing.

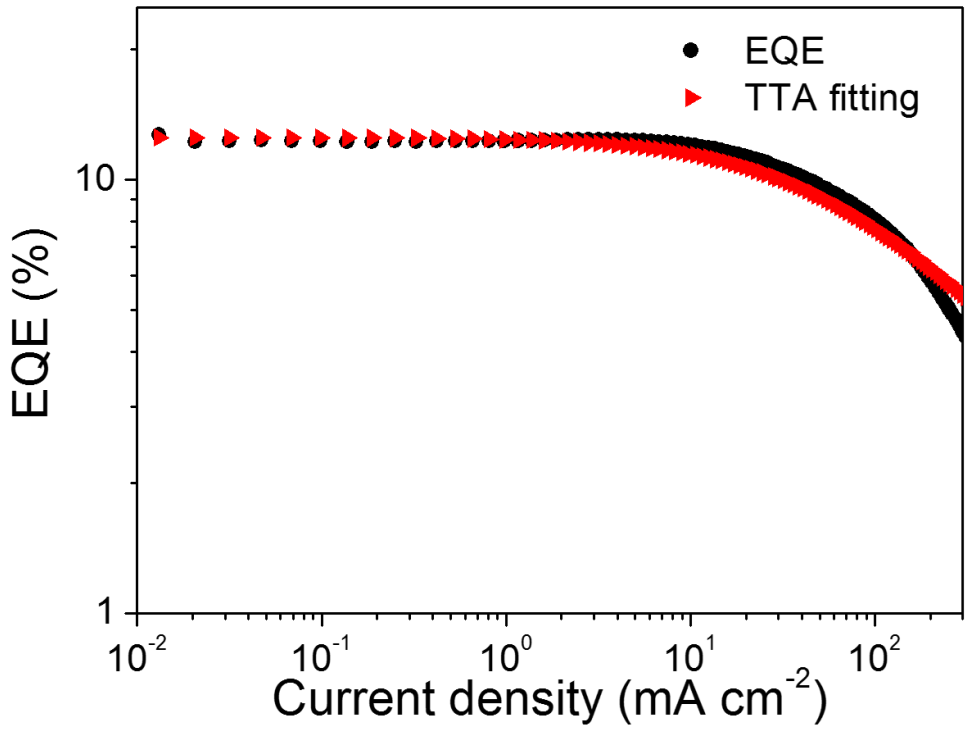

Figure S13. The EQE characteristics with theoretical triplet-triplet annihilation (TTA) fitting.

5. References

S1 M. J. Frisch, G. W. Trucks, H. B. Schlegel, G. E. Scuseria, M. A. Robb, J. R. Cheeseman, G. Scalmani, V. Barone, B. Mennucci, G. A. Petersson, H. Nakatsuji, M. Caricato, X. Li, H. P. Hratchian, A. F. Izmaylov, J. Bloino, G. Zheng, J. L. Sonnenberg, M. Hada, M. Ehara, K. Toyota, R. Fukuda, J. Hasegawa, M. Ishida, T. Nakajima, Y. Honda, O. Kitao, H. Nakai, T. Vreven, J. A. Montgomery, Jr., J. E. Peralta, F. Ogliaro, M. Bearpark, J. J. Heyd, E. Brothers, K. N. Kudin, V. N. Staroverov, R. Kobayashi, J. Normand, K. Raghavachari, A. Rendell, J. C. Burant, S. S. Iyengar, J. Tomasi, M. Cossi, N. Rega, J. M. Millam, M. Klene, J. E. Knox, J. B. Cross, V. Bakken, C. Adamo, J. Jaramillo, R. Gomperts, R. E. Stratmann, O. Yazyev, A. J. Austin, R. Cammi, C. Pomelli, J. W. Ochterski, R. L. Martin, K. Morokuma, V. G. Zakrzewski, G. A. Voth, P. Salvador, J. J. Dannenberg, S. Dapprich, A. D. Daniels, Ö. Farkas, J. B. Foresman, J. V. Ortiz, J. Cioslowski, and D. J. Fox, *Gaussian 09, Revision C.01*. (Gaussian, Inc., 2009).